# LES OF OPEN ROTOR-STATOR FLOW

**Helge I. Andersson and Magne Lygren**[*]
Department of Energy and Process Engineering,
Norwegian University of Science and Technology
7491 Trondheim, Norway
helge.i.andersson@ntnu.no

## ABSTRACT

Computer experiments (LES) of the axisymmetric and statistically steady turbulent flow between a rotating and a fixed disk have been performed. This flow is a representative of the flow in an unshrouded rotor-stator configuration. The flow is characterized only by a local Reynolds number and a local gap ratio, provided that the distance from the rotation axis is sufficiently large so that the flow is fully turbulent.

Five different cases have been considered, two of which may be classified as 'wide-gap' simulations, whereas the others were 'narrow-gap' simulations. In the latter cases, the variation of the tangential mean flow between the disks closely resembled the S-shaped mean velocity profile in a turbulent Couette flow. In the wide-gap cases, however, a nearly homogeneous core region separated the three-dimensional boundary layers adjacent to the rotor and the stator.

It was observed that the degree of three-dimensionality was gradually reduced with the distance from the axis of rotation. The Reynolds shear stress vector and the mean velocity gradient vector became more aligned and the structural parameter increased towards the typical limit 0.15 found in two-dimensional boundary layers. The moment coefficient $C_\theta$ deduced from the statistically averaged tangential wall-friction at the rotor compared excellently with an empirical correlation, whereas $C_\theta$ at the stator side was substantially lower.

## INTRODUCTION

The axisymmetric and statistically steady turbulent flow between a rotating and a fixed disk is a representative of the flow in unshrouded rotor-stator configurations. This flow is among the canonical flows in which three-dimensional boundary layers can be subjected to in-depth explorations, see e.g. the recent review by Johnston & Flack (1986). However, besides its importance from a fundamental point of view, rotor-stator flows are of great practical concern in turbomachinery applications. A comprehensive treatise on flow over free disks in open and closed rotor-stator configurations was presented by Owen & Rogers (1989). Of particular concern for the present study are the findings of Daily & Nece (1960) in their experimental investigation of confined rotor-stator flow. They identified four different flow regimes, depending on the speed of rotation and the gap width, in which the flow was either laminar or turbulent and the boundary layers near the disks were either separated or merged. It is also well established that the flow is laminar near the axis of rotation and

that transition to turbulence takes place at a certain radial position. Moreover, fully turbulent flow is found at smaller radii near the stator than at the rotor side.

This paper reports on an investigation of the flow sufficiently far away from the axis of rotation so that the flow is fully turbulent, i.e. beyond the transition zone, both on the stator and the rotor side. At a given location defined by the distance r from the axis of rotation, the flow is characterized by a local Reynolds number Re and a local gap ratio G. The objective of this numerical study is to explore how these two independent parameters affect the three-dimensional mean flow, the turbulence statistics and the coherent flow structures in an open rotor-stator configuration. The flow field near the rotating disk can be anticipated to resemble the flow in a confined rotor-stator configuration studied experimentally by Itoh et al. (1992). The present large-eddy simulations (LES) represent a continuation of our earlier DNS reported by Lygren & Andersson (2001, 2002). In LES a priori unknown subgrid-scale (SGS) stresses appear in the filtered equations governing the large-scale motions. Here, the SGS stresses are represented by the mixed dynamic SGS model due to Vreman et al. (1994).

## PROBLEM FORMULATION

We consider the shear-driven motion of an incompressible Newtonian fluid between two parallel disks separated a distance s. The lower disk (rotor) at z = 0 is rotating with a constant angular velocity $\omega$, whereas the upper disk (stator) at z = s is fixed. For the sake of affordability, the computational domain consisted of an angular section $\Delta\theta$ between the radial surfaces $r_1$ and $r_2$, as depicted in Figure 1. Here, the inner radius $r_1$ is sufficiently large so that the flow is turbulent throughout the computational domain. At a given location defined by the distance r from the axis of rotation, the flow is characterized by the local Reynolds number $Re_r = r^2\omega/\nu$
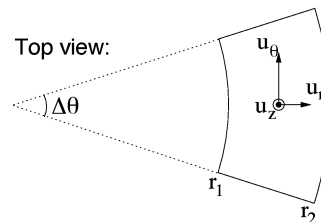


Figure 1: Sketch of the computational domain and coordinate system.

[*]Present address: STATOIL, Forusbeen 50, 4035 Stavanger, Norway

Table 1: Overview of cases considered, domain size and resolution. Case A1 (DNS) has been reported by Lygren & Andersson (2001, 2002) and Case A2 (LES) has been reported and compared with Case A1 by Lygren & Andersson (2004).

| Case | $Re_m$ | $G_m$ | $N_r \times N_\theta \times N_z$ | $L_r/s$ | $L_\theta/s$ | $\Delta r^+$ | $(r_m \Delta\theta)^+$ |
|------|--------|-------|----------------------------------|---------|--------------|--------------|------------------------|
| A1 | $4 \cdot 10^5$ | 0.02 | $192 \times 192 \times 128$ | 3.5 | 7.0 | 5 | 10 |
| A2 | $4 \cdot 10^5$ | 0.02 | $48 \times 96 \times 48$ | 3.5 | 14.0 | 20 | 40 |
| B | $1 \cdot 10^6$ | 0.01265 | $64 \times 96 \times 64$ | 3.5 | 10.0 | 20 | 40 |
| C | $1.6 \cdot 10^6$ | 0.01 | $64 \times 96 \times 64$ | 3.0 | 8.0 | 22 | 38 |
| D | $6.4 \cdot 10^5$ | 0.1 | $128 \times 128 \times 128$ | 1.5 | 3.0 | 24 | 48 |
| E | $1.6 \cdot 10^6$ | 0.0632 | $128 \times 128 \times 192$ | 1.0 | 2.0 | 22 | 44 |

and the local gap ratio $G_r = s/r$, where $\nu$ is the kinematic viscosity of the fluid.

Altogether five different cases have been considered, i.e. five different combinations of the Reynolds number $Re_m = r_m^2 \omega/\nu$ and the gap ratio $G_m = s/r_m$ based on the radial position $r_m = (r_1 + r_2)/2$ of the centre of the computational domain. One particular parameter combination was explored both by DNS (Case A1, Lygren & Andersson 2001, 2002) and LES (Case A2, Lygren & Andersson 2004), while only LESs were performed for the other cases, see Table 1.

## NUMERICAL APPROACH

The three-dimensional Navier-Stokes equations are approximated by second-order accurate central-differences on a staggered grid arrangement and the flow field is advanced explicitly in time using a fractional-step technique and second-order accurate Adams-Bashforth time stepping. The computer code used was originally developed by Gavrilakis et al. (1986). In the course of the present study, the code was recast from Cartesian to cylindrical coordinates. Moreover, the original Poisson solver for the pressure field was replaced by a multigrid technique using repeated V-cycles and Line-Zebra Gauss-Seidel smoothening; cf. Andersson et al. (1998).

No-slip conditions are imposed at the stationary and the rotating disks so that the near-wall regions are explicitly computed. Conventional periodic boundary conditions were employed in the tangential direction, whereas full periodicity could not be assumed in the radial direction. Here, we adopted a modified version of a scheme used by Wu & Squires (2000) in LES of flow over a rotating disk. Their scheme represents a simplification of the boundary treatment devised by Lund et al. (1998) in their simulation of spatially developing boundary layers. The quasi-periodicity imposed in the radial direction in the present study consists of the following basic steps at each time level. First, the instantaneous velocity field is decomposed into mean and fluctuating parts, the latter being formed as the product of root-mean-square of the turbulent fluctuations (averaged in the tangential direction and time) and a time-dependent signal assumed to exhibit periodicity between the coordinate planes $r_1$ and $r_2$. Thereafter, the fluctuating signal is used to generate time-dependent velocity fields at $r_1$ and $r_2$ at the new time level. Finally, global mass conservation is assured by imposition of a zero-mass-flux constraint through the coordinate planes $r_1$ and $r_2$.

In large-eddy simulations, a priori unknown subgrid-scale stresses appear in the filtered equations governing the large-scale motions. The unresolved small-scale turbulence is therefore represented by a subgrid-scale (SGS) model. The eddy-viscosity type SGS model originally implemented in the computer code was here replaced by the dynamic SGS model proposed by Lilly (1992) and the mixed dynamic model due to Vreman et al. (1994). A common feature of these SGS models is that the socalled Smagorinsky coefficient $C_s$ is evaluated as a part of the solution rather than being a prescribed constant. See Lygren & Andersson (2004) for details. In that comparative study it was concluded that the best overall results were obtained with the mixed dynamic SGS model. That model has therefore been adopted in the present parameter study.

For all cases considered, the parameter values, the size of the computational domain, and the numerical resolution are summarized in Table 1. Here, $L_r$ and $L_\theta = r_m\Delta\theta$ denote the length of the domain in the radial and tangential directions, respectively, and $N_i$ is the number of grid points in the $x_i$-direction. In an attempt to achieve about the same resolution in all cases considered, the grid spacings in wall units were about $40 \times 20$ in the $\theta$- and $r$-directions. The grid points next to the disks were about 0.5 wall units away from the surface.

## RESULTS AND DISCUSSION

The two controlling parameters $Re_m$ and $G_m$ can be combined into the gap Reynolds number:

$$Re_G \equiv s^2\omega/\nu = G_m^2 \cdot Re_m \qquad (1)$$

Table 2 shows that $Re_G$ effectively distinguishes between narrow-gap cases (A, B, C) and wide-gap cases (D, E). This table also includes the Reynolds number based on the gap width s and the tangential wall-friction velocity at the rotating $(Re_R^*)$ and the fixed $(Re_s^*)$ disks. The narrow-gap Case A corresponds to the experimental study of Itoh (1995) and comparisons between DNS data and the laboratory measurements were made by Lygren & Andersson (2001). The wide-gap case D corresponds to the case studied by Itoh et al. (1992) and comparisons will be made herein.

The tangential and radial mean velocity components are shown for Cases A - C in Fig. 2 and Cases D - E in Fig. 3. Profiles for the laminar case are included for comparative purposes. The former cases are considered as 'narrow-gap' cases with $Re_G = 160$ (see Table 2), and the tangential velocity exhibits a S-shaped profile similar to that in plane turbulent Couette flow (Bech et al. 1995). In the 'wide-gap' cases in Fig. 3, on the other hand, $Re_G = 6400$ and a nearly homogeneous core region separates the three-dimensional boundary layers adjacent to the rotor and stator. Here, comparisons are also made with the experimental data of Itoh et al. (1992).

It is noteworthy that the tangential velocity is consistently below $0.5\omega r$ midway between the disks. In the narrow-gap
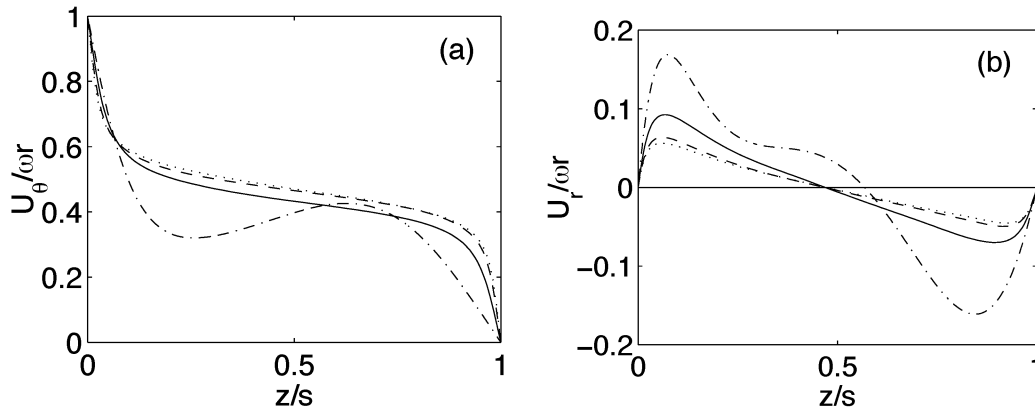
Figure 2: Mean velocity components in tangential (a) and radial (b) direction in the narrow-gap cases. Laminar flow: chain-dotted line; Case A2: solid line; Case B: broken line; Case C: dotted line.
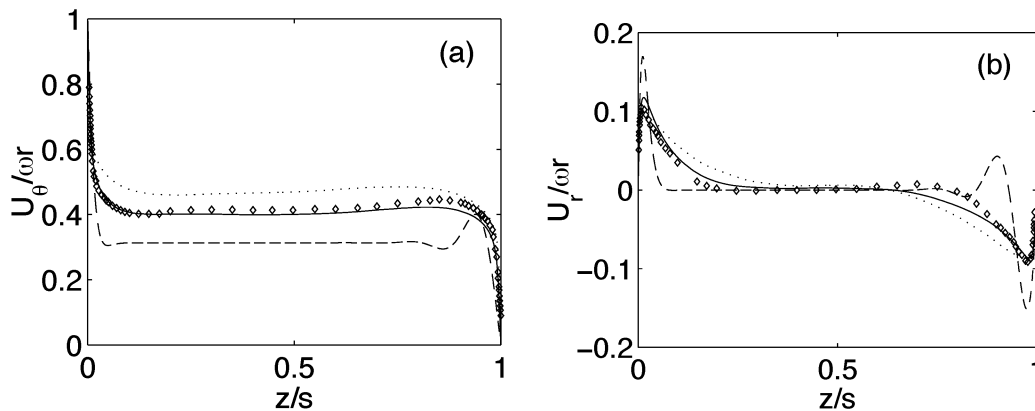


Figure 3: Mean velocity components in tangential (a) and radial (b) direction in the wide-gap cases. Laminar flow: broken line, Case D: solid line; Case E: dotted line; Symbols from Itoh et al. (1992).

Table 2: $Re_R^*$ and $Re_s^*$ based on the tangential wall-friction velocity at the rotor (R) and stator (S).

| Case | $G_m$ | $Re_G$ | $Re_R^*$ | $Re_s^*$ |
|------|-------|--------|----------|----------|
| A1 | 0.02 | 160 | 265.7 | 213.5 |
| A2 | 0.02 | 160 | 267.7 | 214.3 |
| B | 0.01265 | 160 | 381 | 349 |
| C | 0.01 | 160 | 460 | 426 |
| D | 0.1 | 6400 | 2050 | 1534 |
| E | 0.0632 | 6400 | 2856 | 2564 |

cases, $U_\theta/\omega r$ is 0.43, 0.46 and 0.47 in the three different cases and thereby tended towards the plane Couette flow value 0.50 with increasing $Re_m$. The profiles of $U_r$ in Fig 2b shows that the cross-flow reduces with increasing $Re_m$. The reduced three-dimensionality is also reflected by the data in Table 2, i.e. the wall-friction Reynolds numbers at the two disks become gradually closer at the higher $Re_m$. In the wide-gap cases D and E the core velocity was about $0.40\omega r$ and $0.47\omega r$, i.e. substantially larger than $0.31\omega r$ in the laminar case.

Even for a fixed gap Reynolds number, the flow field is affected by the local Reynolds number. Let us for example consider the structural parameter $a_1 = \tau/2k$, where $\tau$

denotes the magnitude of the shear stress vector in the $(r, \theta)$-plane and k is the mean turbulent kinetic energy. Thus, $\tau = (\overline{u_\theta u_z}^2 + \overline{u_r u_z}^2)^{1/2}$ in the present context. The results in Figures 4 and 5 show that $a_1$ approaches the standard value 0.15 for two-dimensional boundary layers away from the disks, except for the lowest Reynolds number cases A and D, for which considerably lower values are observed. The same observations are made both in the narrow-gap and the wide-gap simulations. The observed reduction of $a_1$ indicates that rotor-stator flow is less efficient in extracting turbulence energy from the mean flow.

Alternative measures of the mean flow skewness are the angle between the mean velocity gradient vector $(\partial U_\theta/\partial z, \partial U_r/\partial z)$ and the angle between the shear stress vector $(\overline{u_\theta u_z}, \overline{u_r u_z})$ and the tangential direction, respectively. These angles are shown in Fig. 6 for the three 'narrow-gap' cases, i.e. Cases A-C, for which $Re_G = 160$. These angles are seen to decrease with increasing value of the local Reynolds number both at the rotating and the stationary disk. This reflects that the mean flow is gradually becoming more aligned with the tangential direction.

The dotted lines in Figure 6 represent the misalignment of the mean velocity gradient vector with the shear stress vector. A substantial misalignment of about 20 degrees is observed in the immediate vicinity of the disks as well as far beyond the
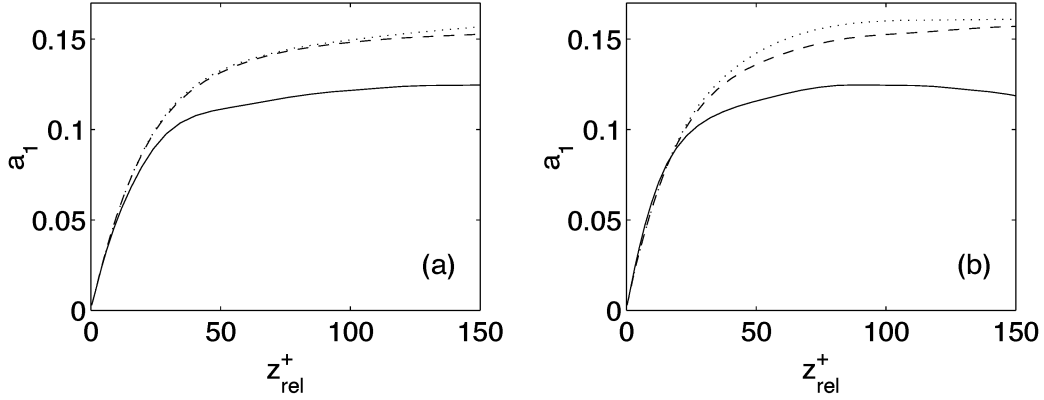
925

Figure 4: Structural parameter $a_1 = \tau/2k$ in the narrow-gap cases. Rotor (a) and stator (b) side. Legend as in Fig. 2.
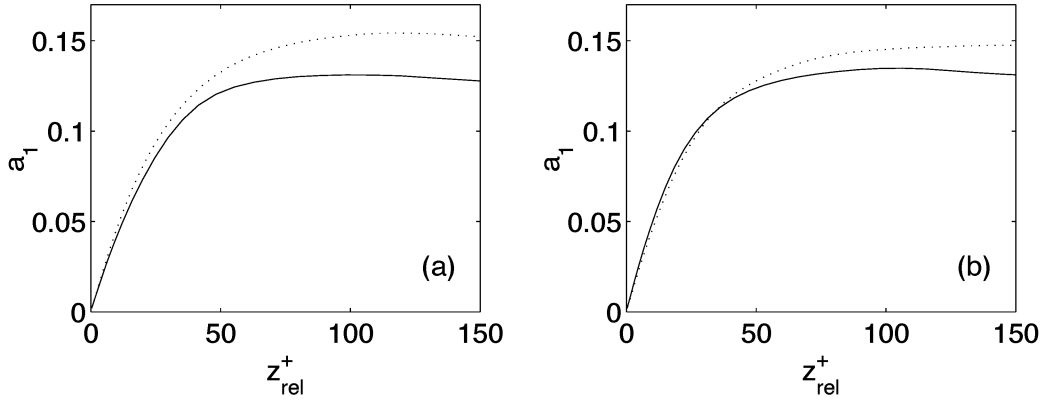


Figure 5: Structural parameter $a_1 = \tau/2k$ in the wide-gap cases. Rotor (a) and stator (b) side. Legend as in Fig. 3.

buffer region. Since isotropic eddy viscosity models rely on a perfect alignment of the shear stress vector with the velocity gradient vector, such closures are likely to fail in rotor-stator flows. It is noteworthy that this misalignment persists also at the higher $Re_m$ cases B and C, even though the structure parameter $a_1$ attains its conventional value 0.15 in these cases; cf Figure 4. Similar observations were made also for the wide-gap cases D and E (not shown here due to space limitations).

The tangential component of the skin-friction vector is directly responsible for the torque exerted by the fluid on the two disks. According to the Reynolds numbers based on the wall-friction in Table 2, the tangential component of the wall friction on the rotating disk (rotor) is generally higher than on the fixed disk (stator). Daily & Nece (1960) provided an empirical correlation for the torque coefficient for narrow-gap cases. From that correlation, the following correlation for the skin-friction drag coefficient $C_\theta = 2\tau_\theta/\rho(r\omega)^2$, where $\tau_\theta$ denotes the tangential component of the skin-friction vector, can be deduced:

$$C_\theta = 0.0298 G_r^{-1/6} Re_r^{-1/4} \tag{2}$$

Here, $Re_r$ and $G_r$ denote local Reynolds number and gap ratio (see Problem Formulation). The correlation (2) is shown in Figure 7 together with the present LES data. The wall friction at the rotor (stars) closely follows the empirical line (2), whereas the flow resistance turns out to be lower at the stator side (squares). It can be anticipated that the radial mean velocity component will be further reduced at even higher $Re_r$

and the friction at the two disks will eventually become equal. The LES data for the wide-gap cases in Figure 8 show a somewhat bigger difference between the rotor and the stator. Here, the experimental data of Itoh et al. (1992) show the same trend as the computer experiments.

**CONCLUDING REMARKS**

This parameter study has demonstrated the distinguishing features of narrow-gap and wide-gap rotor-stator configurations. In spite of the fundamentally different core regions, the three-dimensional flow fields in the vicinity of the two disks exhibit the same general features in all cases considered.

The present study supports the view advocated by Littell & Eaton (1994) that the mean flow three-dimensionality affects the near-wall vortices and their ability to generate shear stresses. This conclusion applies both for the narrow-gap and the wide-gap cases. The difference between the rotor and the stator sides diminishes with increasing local Reynolds number. A separate analysis of conditionally averaged shear stresses (Andersson & Lygren 2002) supports these findings.
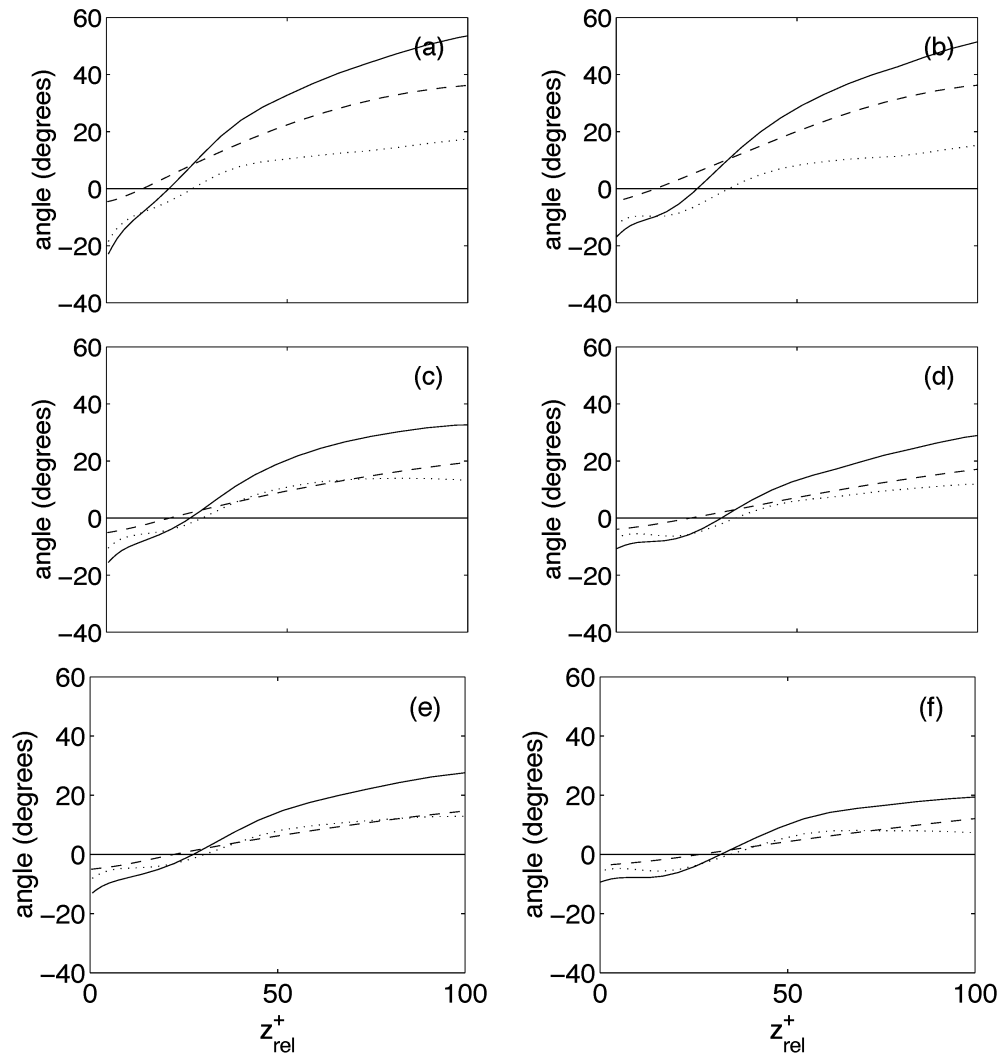
Figure 6: Mean gradient angle (solid lines); shear stress angle (broken lines); difference (dotted lines). Rotor side (left) and stator side (right). Case A2: (a) and (b); Case B: (c) and (d); Case C: (e) and (f).
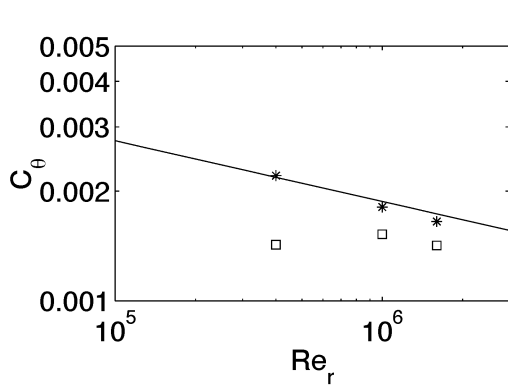


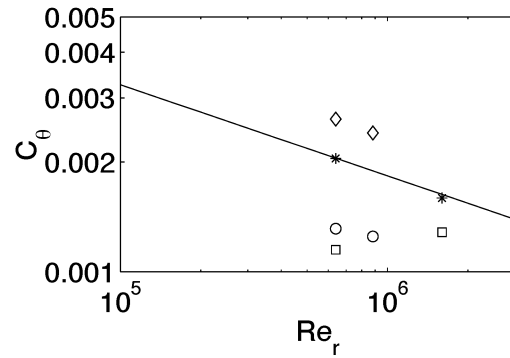Figure 7: Friction factor at the rotor ($\star$) and stator ($\square$) Case A2, B and C.

Figure 8: Friction factor at the rotor ($\star$) and stator ($\square$) Case D and E. Data from Itoh et al. (1992): rotor ($\diamond$) and stator ($\circ$).

## REFERENCES

Andersson, H.I., and Lygren, M., 2002, "Coherent structures in 3D mean flow", *Advances in Turbulence IX*, I.P. Castro et al., eds., CIMNE, pp. 649-652.

Andersson, H.I., Lygren, M., and Kristoffersen, R., 1998, "Roll cells in turbulent plane Couette flow: reality or artifact?", *16th International Conference on Numerical Methods in Fluid Dynamics*, C.H. Bruneau, ed., Springer, pp. 117-122.

Bech, K.H., Tillmark, N., Alfredsson, P.H., and Andersson, H.I., 1995, "An investigation of turbulent plane Couette flow at low Reynolds numbers", *Journal of Fluid Mechanics*, Vol. 286, pp. 291-325.

Daily, J.W., and Nece, R.E., 1960, "Chamber dimension effects on induced flow and frictional resistance of enclosed rotating disks", *ASME Journal of Basic Engineering*, Vol. 82, pp. 217-232.

Gavrilakis, S., Tsai, H.M., Voke, P.R., and Leslie, D.C., 1986, "Large-eddy simulation of low Reynolds number channel flow by spectral and finite difference methods", *Notes on Numerical Fluid Mechanics*, Vol. 15, U. Schumann and R. Friedrich, eds., Vieweg, pp. 105-118.

Itoh, M., 1995, "Experiments on the turbulent flow in the narrow clearance between a rotating and a stationary disk", *Turbulent Flows*, B.F. Carrol et al., eds., ASME-FED, Vol. 208, pp. 27-32

Itoh, M., Yamada, Y., Imao, S., and Gonda, M., 1992, "Experiments on turbulent flow due to an enclosed rotating disk", *Experimental Thermal and Fluid Sciences*, Vol. 5, pp. 359-368.

Johnston, J.P., and Flack, K.A., 1996, "Review - advances in three dimensional turbulent boundary layers with emphasis on the wall-layer regions", *ASME Journal of Fluids Engineering*, Vol. 118, pp. 219-232.

Lilly, D.K., 1992, "A proposed modification of the Germano subgrid-scale closure method", *Physics of Fluids*, Vol. A4, pp. 633-635.

Littell, H.S., and Eaton, J.K., 1994, "Turbulence characteristics of the boundary layer on a rotating disk", *Journal of Fluid Mechanics*, Vol. 266, pp. 175-207.

Lund, T.S., Wu, X., and Squires, K.D., 1998, "Generation of turbulent inflow data for spatially developing boundary layer simulations", *Journal of Computational Physics*, Vol. 140, pp. 233-258.

Lygren, M., and Andersson, H.I., 2001, "Turbulent flow between a rotating and a stationary disk", *Journal of Fluid Mechanics*, Vol. 426, pp. 297-326.

Lygren, M., and Andersson, H.I., 2002, "Turbulence statistics in an open rotor-stator configuration", *Physics of Fluids*, Vol. 14, pp. 1137-1145.

Lygren, M., and Andersson, H.I., 2004, "Large eddy simulations of the turbulent flow between a rotating and a stationary disk", Zeitschrift für angewandte Mathematik und Physik, Vol. 55, pp. 268-281. First version in *Proceedings 2nd International Symposium on Turbulence and Shear Flow Phenomena*, E. Lindborg et al., eds., KTH, Stockholm (2001), pp. 407-412.

Owen, J.M., and Rogers, R.H., 1989, Flow and Heat Transfer in Rotating-Disk Systems: Rotor-Stator Systems, Research Studies Press, Taunton, NY.

Vreman, B., Geurts, B., and Kuerten, H, 1994, "On the formulation of the dynamic mixed subgrid-scale model", *Physics of Fluids*, Vol. 6, pp. 4057-4059.

Wu, X., and Squires, K.D., 2000, "Prediction and investigation of the turbulent flow over a rotating disk", *Journal of Fluid Mechanics*, Vol. 418, pp. 231-264.